

See discussions, stats, and author profiles for this publication at: <https://www.researchgate.net/publication/26782276>

Gold Nanoparticles Functionalized with Gadolinium Chelates as High-Relaxivity MRI Contrast Agents

ARTICLE in JOURNAL OF THE AMERICAN CHEMICAL SOCIETY · SEPTEMBER 2009

Impact Factor: 12.11 · DOI: 10.1021/ja904094t · Source: PubMed

CITATIONS

76

READS

85

6 AUTHORS, INCLUDING:



Caroline Cannizzo

Université d'Évry-Val-d'Essonne

17 PUBLICATIONS 395 CITATIONS

SEE PROFILE



Cédric R Mayer

Université de Versailles Saint-Quentin

64 PUBLICATIONS 2,763 CITATIONS

SEE PROFILE



Lothar Helm

École Polytechnique Fédérale de Lausanne

240 PUBLICATIONS 7,685 CITATIONS

SEE PROFILE

Gold Nanoparticles Functionalized with Gadolinium Chelates as High-Relaxivity MRI Contrast Agents

Loïck Moriggi,[†] Caroline Cannizzo,[†] Eddy Dumas,[‡] Cédric R. Mayer,^{*,§} Alexey Ulianov,[§] and Lothar Helm^{*,†}

Institut des Sciences et Ingénierie Chimique, Ecole Polytechnique Fédérale de Lausanne (EPFL), CH 1015 Lausanne, Switzerland, Institut Lavoisier de Versailles, UMR 8180 CNRS, 45 avenue des Etats-Unis, F 78035 Versailles, France, and Institut de Minéralogie et Géochimie, Université de Lausanne, CH 1015 Lausanne, Switzerland

Received May 20, 2009; E-mail: lothar.helm@epfl.ch

Functionalized nanoparticles (NPs) are presently under intensive study aimed at creating useful tools for molecular diagnosis, therapy, and biotechnology.^{1,2} Especially, applications in magnetic resonance molecular imaging (MRI), which suffer from the intrinsically low sensitivity of this technique, rely on the development of efficient contrast agents.^{3–5} If we consider gadolinium-based agents, the efficiency can be augmented by increasing the relaxation enhancement induced by a single paramagnetic Gd³⁺ ion and by bringing a large number of these ions to the molecular target. From theoretical considerations, a relaxation enhancement (relaxivity) of $\sim 100 \text{ mM}^{-1} \text{ s}^{-1}$ induced by 1 mM Gd³⁺ can be expected as a maximum for T₁ contrast agents.³ However, the number of Gd³⁺ ions that can be delivered to a specific volume element is not restricted by stringent physics rules but by the challenging synthesis of complex compounds and more soft biological and chemical limitations.

A route for creating nanosized units that can be loaded with chelating ligands involves nanocrystals made of noble metals such as gold or silver. Gold NPs are easily functionalized by thiol derivatives, opening multimodal perspectives. To design a potential MRI contrast agent, nanocrystals coated with Gd³⁺ chelates present the advantage of a rigid core that minimizes internal degrees of freedom. Another interesting aspect is the high electron density of these heavy-metal objects, promising gold NPs as agents for X-ray imaging.^{4–7}

Recent studies have revealed that gold NPs show intrinsic magnetization of Au in thiol-capped gold NPs with a permanent magnetism at room temperature.^{8–12} With respect to MRI, it is conceivable that the metallic core of an NP coated with gadolinium chelate thiol derivatives can contribute to the relaxivity of the bulk water molecules, in addition to the contribution from the electron spin of the Gd³⁺ ions.

In the present study, a thiol derivative DTTA¹³ chelate (called Dt) was used as the protective agent for the Au NPs. Batches of gold Dt-coated NPs (DtNP) were synthesized using different HAuCl₄/Dt ratios [Table S1 in the Supporting Information (SI)]. DtNPs were complexed with gadolinium(III) and yttrium(III) by mixing solutions of DtNPs with a slight excess of aqueous solutions of LnCl₃ (Ln = Gd, Y). The resulting solutions were filtered with a 0.2 μm hydrophilic syringe filter and purified with a size-exclusion chromatography column (Sephadex LH20). Gold, gadolinium, and yttrium concentrations in solution were determined by ICP–MS analysis. In parallel, different dilutions of the Gd–DtNP solution ([Gd] from 201 to 34 μM) were analyzed, and a mean Au/Gd-ratio

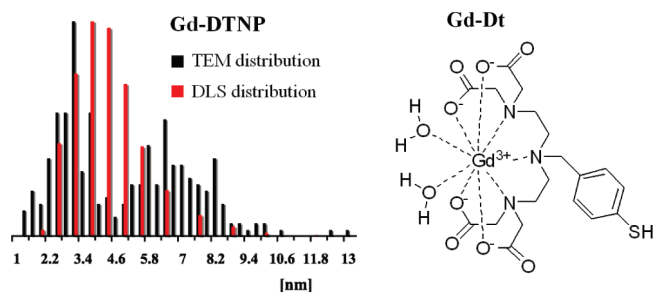


Figure 1. (left) Diameter size distributions obtained from (black) TEM images and (red) DLS. (right) Chelating unit Dt complexed with gadolinium (Gd–Dt).

of 3.6 was measured. The Gd–DtNP solutions were further analyzed using scanning transmission electron microscopy coupled to energy-dispersive X-ray analysis (STEM–EDX; see Figure S2 in the SI).

Size distributions were determined from Feret's diameters (Figure 1, black histogram) of particles obtained from TEM images (Figure S1 in the SI) and dynamic light scattering (DLS; Figure 1, red histogram). It has to be kept in mind that the TEM distribution was obtained from a deposit of particles on a carbon-coated copper grid while the DLS distribution represents the hydrodynamic diameter in solution. The distribution from DLS is narrower, but the overall accordance between the results is good. From the distributions, we calculated a mean particle diameter of 4.8 nm.

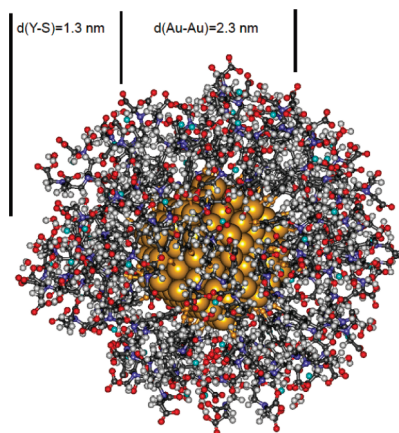


Figure 2. Partially optimized structure (MM3 force field) of Y–DtNP containing 201 gold atoms, 56 Y–Dt chelates, and 112 water molecules.

To obtain a microscopic picture of our functionalized gold NPs, we used partially optimized molecular mechanics with the MM3

[†] Ecole Polytechnique Fédérale de Lausanne.

[‡] Université de Versailles.

[§] Université de Lausanne.

force field, as implemented in the Scigress Explorer 7.7 program. Barnard et al.¹⁴ found evidence for the formation of a discrete sequence of truncated octahedral morphological motifs for gold NPs over 1.5 nm. The particle formed is therefore described by the formula $\text{Au}_{201}[\text{Y-Dt}(\text{H}_2\text{O})_2]_{56}$ (Figure 2). The Au/Y ratio used was 3.6, corresponding to the mean Au/Gd ratio determined by ICP-MS.

Visual inspection of a space-filling model (see Figure S4 in the SI) shows that the spherical shell formed by the Y-Dt chelates is densely packed. From the simple model, it can be deduced that the thickness of the spherical shell is 1.3 ± 0.3 nm, corresponding in this particular case roughly to the radius of the gold core. The total diameter of the modeled particle is ~ 4.9 nm and corresponds to the mean diameter of the Gd-DtNP measured by DLS.

Thiol-covered gold nanoparticles are known to show magnetic behavior.¹¹ In view of the goal of creating particles that potentially can act as MRI contrast agents, any magnetic property of the particle is of natural interest. We determined the effective magnetic moment (μ_{eff}) per gadolinium ion in different dilutions of Gd-DtNP by ^1H NMR analysis using Evans' method.^{15,16} The μ_{eff} values of the solutions obtained from the experimental chemical shifts (Table S2 in the SI) are in close accordance with the effective magnetic moment of Gd^{3+} [$\mu_{\text{eff}}(\text{Gd}^{3+}) = 7.94$]. No magnetic moment was detected from ^1H NMR shifts of the Y-DtNP solution, even at the high magnetic field of 18.8 T. The gold core of the NP therefore does not contribute significantly to the overall magnetic moment of Gd-DtNPs.

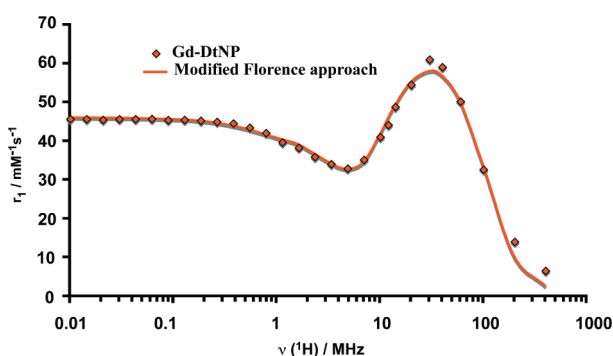


Figure 3. ^1H NMRD profile for Gd-DtNPs at 298 K and the fit using the modified Florence approach.

The nuclear magnetic relaxation dispersion (NMRD) profiles of Gd-DtNP were measured at 25 °C (Figure 3). Both Gd-DtNP batches led to very similar relaxivities (r_1). A very high relaxivity maximum of $\sim 60 \text{ mM}^{-1} \text{ s}^{-1}$ at 30 MHz was found, corresponding to a relaxation enhancement per NP of more than $3000 \text{ mM}^{-1} \text{ s}^{-1}$. Tillement⁶ and Kim⁷ both used ligands chelating several Gd^{3+} ions, leading to lower relaxivities but higher relaxation enhancements per NP. Various theoretical approaches have been developed to analyze NMRD profiles of gadolinium compounds.¹⁷ We used the approach of Bertini et al.¹⁸ and Kruk et al.,¹⁹ which has been implemented in the software package developed in Florence and is called the “modified Florence method”.²⁰ This method is well-suited for fitting the experimental NMRD profiles for slowly rotating complexes of gadolinium(III), with a $S = 7/2$ ion characterized by relatively low static zero-field splitting (ZFS).

The data fitting was performed by fixing most of the parameters to values typical for Gd complexes with the DTTA chelating unit. The four parameters fitted were the overall rotational correlation time (τ_R^{298}), the correlation time for the transient ZFS (τ_v^{298}), and the amplitudes of the transient and static ZFS (Δ_t^2 and Δ_s^2 ,

respectively) (Table S3 in the SI). The results for the transient ZFS are close to the values found for the Ru-based metallostear $\{\text{Ru}[\text{Gd}_2\text{bpy-DTTA}_2(\text{H}_2\text{O})_4]_3\}^{4-}$,²¹ which is built using the same chelating unit. However, the amplitude of the static ZFS is $\sim 30\%$ lower than that for $\{\text{Ru}[\text{Gd}_2\text{bpy-DTTA}_2(\text{H}_2\text{O})_4]_3\}^{4-}$. A global rotational correlation time $\tau_R^{298} = 1.2 \text{ ns}$ was calculated for Gd-DtNPs. The dense packing of the Gd-Dt units on the surface of the NPs makes them very rigid. The absence of internal rotation of the Gd-chelating units leads to a very good fit, even at high NMR frequencies ($\nu \geq 200 \text{ MHz}$).

In conclusion, we have developed small, stable, water-dispersible, DTTA thiol-functionalized gold NPs complexed with paramagnetic gadolinium or diamagnetic yttrium rare-earth ions. Characterizations using TEM images, DLS, and STEM-EDX analysis indicated a particle size distribution from 1 to 13 nm. Bulk magnetic susceptibility measurements at high magnetic field showed the absence of a significant magnetic contribution from the gold core. NMRD profiles of Gd-DtNP solutions at 25 °C showed very high relaxivities with marked relaxivity humps between 10 and 60 MHz, indicating slow rotational motion.

Acknowledgment. This work was supported by the Swiss NSF and the French Agence Nationale de la Recherche (ANR-07-JCJC-0040) and was performed in the frame of the EU COST Action D38. We thank Prof. Hon. André Merbach and Dr. Alain Borel for very helpful discussions and Dr. Marco Cantoni and Anas Mouti for TEM images and the STEM-EDX experiment.

Supporting Information Available: Tables S1–S3 and Figures S1–S5. This material is available free of charge via the Internet at <http://pubs.acs.org>.

References

- (1) McCarthy, J. R.; Weissleder, R. *Adv. Drug Delivery Rev.* **2008**, *60*, 1241–1251.
- (2) Debbage, P.; Jaschke, W. *Histochem. Cell Biol.* **2008**, *130*, 845–875.
- (3) Caravan, P.; Farrar, C. T.; Frullano, L.; Uppal, R. *Contrast Med. Mol. Imaging* **2008**, *4*, 89–100.
- (4) Hainfeld, J. F.; Dilmanian, F. A.; Slatkin, D. N.; Smilowitz, H. M. *J. Pharm. Pharmacol.* **2008**, *60*, 977–985.
- (5) Debouttiere, P.-J.; Roux, S.; Vocanson, F.; Billotey, C.; Beuf, O.; Favre-Reguillon, A.; Lin, Y.; Pellet-Rostaing, S.; Lamartine, R.; Perriat, P.; Tillement, O. *Adv. Funct. Mater.* **2006**, *16*, 2330–2339.
- (6) Alric, C.; Taleb, J.; Le Duc, G.; Mandon, C.; Billotey, C.; Le Meur-Herland, A.; Brochard, T.; Vocanson, F.; Janier, M.; Perriat, P.; Roux, S.; Tillement, O. *J. Am. Chem. Soc.* **2008**, *130*, 5908–5915.
- (7) Park, J.-A.; Reddy, P. A. N.; Kim, H.-K.; Kim, I.-S.; Kim, G.-C.; Chang, Y.; Kim, T.-J. *Bioorg. Med. Chem. Lett.* **2008**, *18*, 6135–6137.
- (8) Carmeli, I.; Leitens, G.; Naaman, R.; Reich, S.; Vager, Z. *J. Chem. Phys.* **2003**, *118*, 10372–10375.
- (9) De La Fuente, J. M.; Alcántara, D.; Eaton, P.; Crespo, P.; Rojas, T. C.; Fernández, A.; Hernando, A.; Penadés, S. *J. Phys. Chem. B* **2006**, *110*, 13021–13028.
- (10) Guerrero, E.; Rojas, T. C.; Multigner, M.; Crespo, P.; Muñoz-Marquez, M. A.; García, M. A.; Hernando, A.; Fernández, A. *Acta Mater.* **2007**, *55*, 1723–1730.
- (11) Garitaonandia, J. S.; Insausti, M.; Goikolea, E.; Suzuki, M.; Cashion, J. D.; Kawamura, N.; Ohsawa, H.; De Muro, I. G.; Suzuki, K.; Plazaola, F.; Rojo, T. *Nano Lett.* **2008**, *8*, 661–667.
- (12) Crespo, P.; Guerrero, E.; Muñoz-Marquez, M. A.; Hernando, A.; Fernández, A. *IEEE Trans. Magn.* **2008**, *44*, 2768–2771.
- (13) Moriggi, L.; Cannizzo, C.; Prestinari, C.; Berrière, F.; Helm, L. *Inorg. Chem.* **2008**, *47*, 8357–8366.
- (14) Barnard, A. S.; Curtiss, L. A. *ChemPhysChem* **2006**, *7*, 1544–1553.
- (15) Evans, D. F. *J. Chem. Soc.* **1959**, 2003–2005.
- (16) Evans, D. F.; Fazakerley, G. V.; Phillips, R. F. *J. Chem. Soc. A* **1971**, 1931–1934.
- (17) Kowalewski, J.; Kruk, D.; Parigi, G. *Adv. Inorg. Chem.* **2006**, *57*, 41–104.
- (18) Bertini, I.; Kowalewski, J.; Luchinat, C.; Nilsson, T.; Parigi, G. *J. Chem. Phys.* **1999**, *111*, 5795–5807.
- (19) Kruk, D.; Nilsson, T.; Kowalewski, J. *Phys. Chem. Chem. Phys.* **2001**, *3*, 4907–4917.
- (20) Bertini, I.; Galas, O.; Luchinat, C.; Parigi, G. *J. Magn. Reson.* **1995**, *113A*, 151–158.
- (21) Moriggi, L.; Aebischer, A.; Cannizzo, C.; Sour, A.; Borel, A.; Bünzli, J. C.; Helm, L. *Dalton Trans.* **2009**, 2088–2095.

JA904094T